.

EXPERIMENTAL INVESTIGATION OF RAMP INJECTION INTO SUPERSONIC CROSSFLOW USING NANOPARTICLE-BASED PLANAR LASER SCATTERING

LIU Weidong *, ZHANG Shunping *
*** College of Aerospace and Material Engineering, National Univ. of Defense Technology, Changsha, China, 410073**

Keywords: *NPLS, ramp injector, mixing enhancement, stream-wise vortices*

Abstract

Nanoparticle-based Planar Laser Scattering (NPLS) method and other nonintrusive optical diagnostic techniques have been employed in an experimental investigation of the flowfield downstream of ramp injection system in a scramjet combustor. The high enthalpy supersonic air crossflow is at Mach 2.0, and the fuel is simulated by nitrogen injected at Mach 1.0. Mixing the injection nitrogen gas with nanoparticles, the fuel distribution and instantaneous displacement demonstrated by the nanoparticles are imaged with laser sheet scattering measurement. The NPLS method which gives clear identification of the jet/mainstream interface in each of the three visualized cross planes and in the side views has proved to be a successful flow visualization technique for three-dimensional supersonic flow. Mixing characteristics of ramps with different geometries are inferred from image analysis. The results indicate that the mixing process is dominated by the ramp-generated streamwise vortices. It is also found that the sweepback configuration strengthens the streamwise vortices greatly and the reflected oblique shock projecting onto the injection plume can intensify mixing effectively.

1 Introduction

Hypersonic vehicles will play an important role in air and space transportation for the foreseeable future. As a promising candidate propulsion system, the supersonic combustion ramjet engine (SCRAMJET engine) has being actively researched around the world.[1] Because of the extremely short residence time of the fuel in the combustor and the low growth rate of the supersonic turbulent mixing layer, mixing enhancement constitutes a critical factor in the design of scramjet engines. Various methods including transverse injection from the wall, shock-enhanced mixing by generation of baroclinic torque, generation of axial vorticity of the airstream using pylon-aided fuel injectors, and generation of streamwise vorticity using alternating wedges, have been explored in an attempt to enhance the fuel–air mixing rate[2].

Ramp injector as an effective mixing enhancement flush-wall injector has been studied extensively recent years.[3]-[12] These injectors generate vortices when crossflow is compressed by the top of the ramp and spills over the ramp corners into the lower-pressure region among the ramps. The effect enhanced by sweeping the ramp side walls so that the region between the ramps diverges streamwise, causes the air in between to accelerate and expand to a lower pressure.

The main purpose of this investigation is to conduct a detailed study of the complex three-dimensional flowfield generated by the ramp injector configuration employing the advanced nonintrusive optical diagnostic techniques. On the basis of flowfield mapping， the mixing efficiency through the use of different ramp geometries is evaluated.

2 Experimental Descriptions

2.1 Test Facility

The experimental facility can be seen in Fig 1. The model scramjet combustor is directly installed behind the nozzle of the air heater

which heats the air by means of air/O2/H2

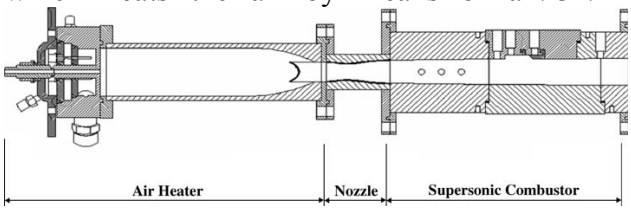

Fig. 1 Schematic of experimental facility

combustion. Flow condition of nozzle exit are listed in Table 1 and the O2 mass fraction is 23.3% in the vitiated air. The cross-sectional area is 32.6 × 44 mm at the exit of the facility nozzle. The test section, with constant width of 44 mm, is connected directly to the exit of the facility nozzle. The test section has an expand angle of 2◦ on top wall side. The ramp injectors are mounted on the bottom side. The whole length of the combustor (test section) is 400 mm. Three quartz glass windows are mounted on the combustor to transfer plane beam.

Table. 1 Inflow conditions

	Nozzle exit
Stagnation temperature (T_0), K	1221
Static temperature (T), K	780
Ratio of specific heats (γ)	1.34
Stagnation pressure (P_0), MPa	0.5
Mach number (M)	2.0

2.2 Measurement Techniques

The NPLS (Nanoparticle-based Planar Laser Scattering) method[13] has been used as the primary flow diagnostic in this investigation, which is mainly composed by computer, synchronizer, CCD camera, pulse laser and nanoparticle generator, the structure of which is schematically shown in Fig. 2. Due to the good flow-following ability of nanoparticles, the particle distribution will well reflect the mixing structures of the flow field. The nanoparticle generator is driven by high pressure nitrogen gas. To measure the flow field with NPLS, the nanoparticles are injected into and mixed with the injection nitrogen jet. When the flow is established in the test section, the synchronizer controls the laser pulse and CCD to ensure synchronization of the emission of scattering laser by nanoparticles and the double exposures of CCD. Thus NPLS system can also study the temporal evolution of the flow field at time interval between double exposures.

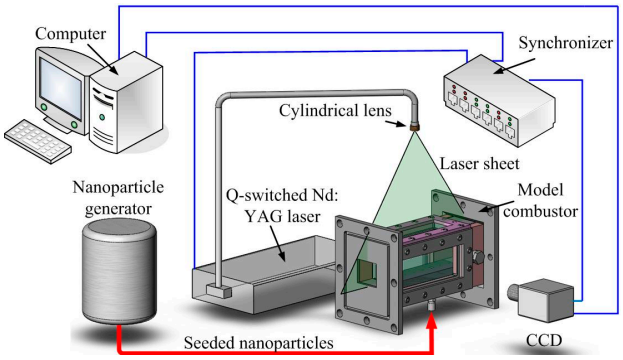

Fig. 2 NPLS (Nanopaticle planar laser scattering) optical arrangement

In Fig 3, the timing diagrams of the synchronizer for the laser pulse and the CCD are shown. The synchronization of the laser and the CCD is controlledby the trigger signal. During NPLS working period, the CCD shutter is triggered by the synchronizer signal and the feedback signal of CCD is transferred back to the synchronizer. At the same time the first frame of CCD exposes. By setting appropriate pulse delay time, the laser emits the first pulse to illuminate nanoparticles in the flow field while CCD is exposing. When the scattered laser lights are captured by CCD, the instantaneous flow structure is recorded. While storing the first image, the second frame of CCD exposes. In the second exposure interval, the second laser pulse emits, and the second particle-image is captured and stored. It can be seen from fig.3 that if the influence of background light is eliminated, the actual exposure time of CCD is just the duration of laser pulse; therefore the lagging phenomenon of particles in supersonic flowfield can be avoided. With these methods, the NPLS system can both measure the instantaneous spatial structures and study the temporal evolution of the flow field at time interval between double exposures. The synchronizer has eight output ports with temporal precision at 0.25ns. The CCD is an interline transfer CCD equipped with micro-lens, of which the frame straddle time is adjustable (the shortest is 200ns) and is set as 5μs in this study. The number of CCD array is 2000×2000 pixels with 4096 grayscale grades. The pulse laser is a double pulse Nd:YAG laser, the wavelength of the laser is 532nm with duration of 6ns and 350mJ per pulse. The location of light sheet lens and the polarization of laser can be adjusted according to experimental requirements.

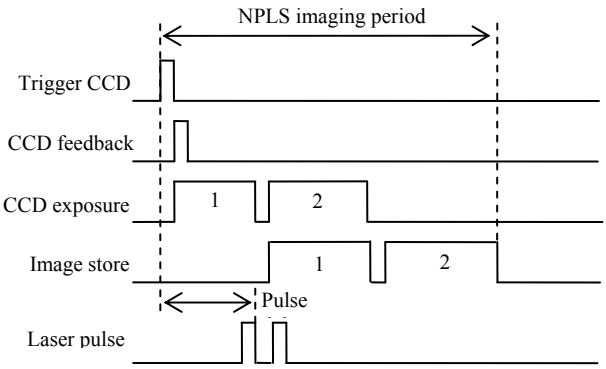

Fig. 3 The Timing diagrams of NPLS

Besides the NPLI method, a conventional Z-Type 2-Mirror Schlieren system and Surface Oil-Flow Visualization technique are combined for mapping the three-dimensional flowfield of the supersonic ramp injectors in this study.

2.3 Ramp Injector Geometries

Fig 4 shows four ramp injector models used in this study. Expansion ramp and compression ramp are shown in Fig. 4. a. The expansion and compression angles are 10 deg and the ramp side walls are swept at 10 deg. Geometries of unswept ramp and swept ramp are shown in Fig. 4. b. They both have a 5 deg expansion angle and a 5 deg compression angle, the swept ramp have a 10 deg sweep angle.The injection plane of all ramp injectors is rectangle, the height and the width of which is respectively 7.3mm and 7mm. Diameter of injection port of all ramps is 1mm.

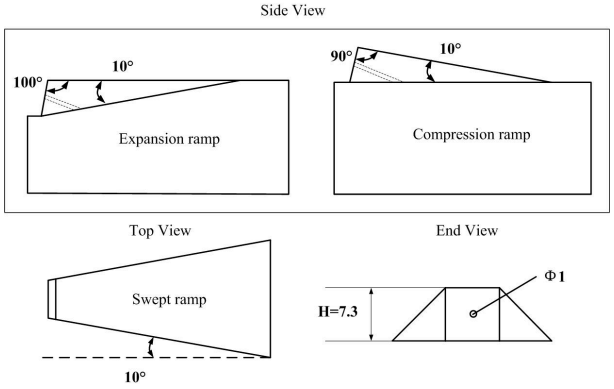

(a) Expansion Ramp and Compression Ramp

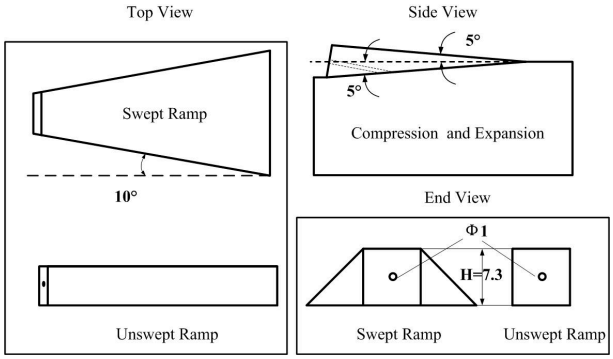

(b) Swept Ramp and Unswept Ramp

Fig. 4 Ramp geometry schematics

3 Results and Discussion

Fig 5 illustrates the image plane orientation that applies to all the NPLS images presented in this study. For spanwise view (profile) images, the laser sheet is directed down through the top wall window and centered on the injection centerline; imaging occurred normal to the sheet through a side wall window. For streamwise (end) views, the sheet is transmitted over the test section span through the side wall windows, and imaging takes place from a side window as well. Streamwise planes measurements are taken at 3 cross-sectional locations X downstream of the injection ports. The location closest to the injection port is at X/H=1.16, where H is the height of the ramp. The streamwise sectional view images are corrected for the view angle distortion of the camera-mirror system by spatially transforming (warping) them using a reference grid taken during the test. The transformed images look as it would have appeared in a perpendicular imaging arrangement. For observation convenience, the NPLS image obtained are dealt with reversing the color.

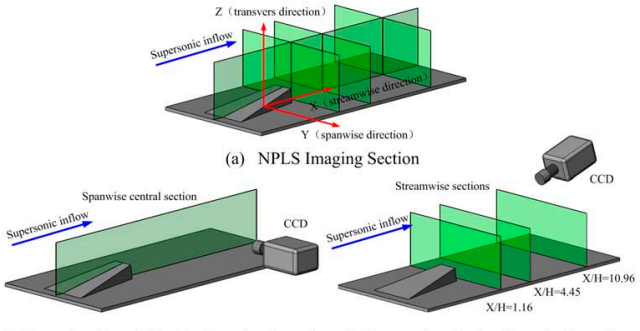

(b) Spanwise Central Section Imaging Location (c) Streamwise Section Imaging Locations

Fig. 5 Schematic illustrating the NPLS image-plane orientation system

3.1 Mixing characteristic comparisons between expansion and compression ramp injectors

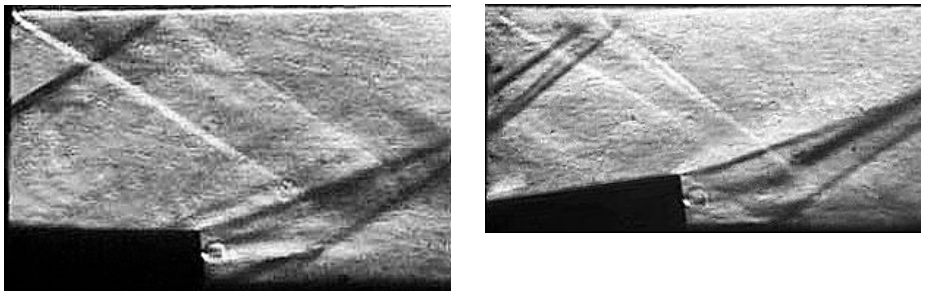

a. Expansion ramp injector **b.** Compression ramp injector

Fig. 6 Schlieren photograph of expansion and compression ramp

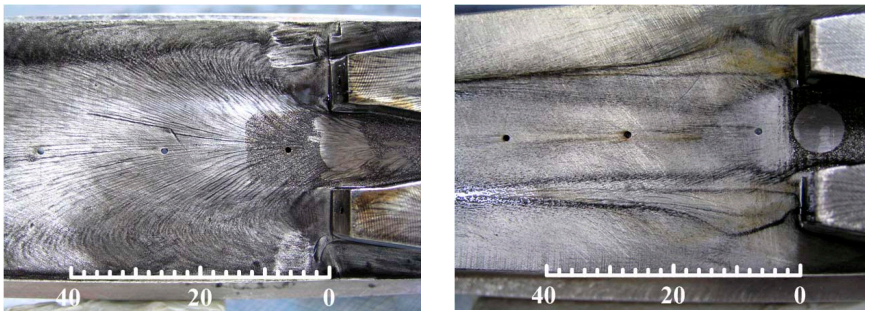

a. Expansion ramp injector **b.** Compression ramp injector

Fig. 7 Oil surface flow pictures of expansion and compression ramp injectors

Fig.6 gives the schlieren photograph and Fig.7 gives the Oil surface flow pictures of expansion and compression ramp. From Fig 6 a and Fig 7 a, it is seen that the oil surface flow image is not apparent, which means that the intensity of streamwise vortices are not large due to the non-enough development. From Fig 7, it is seen that the oilflow image of the compression ramp is completely different from that of the expansion ramp. The injected gas expands quickly from the injection orifice, and are compressed by the side flows around the ramp. The wall flow streamlines begin to converge around the symmetric centerline, further collide with forming a diamond shape, and finally unite to a single line. The phenomena reveal that the streamwise vortices downstream of the compression ramp has generated and sufficiently developed. The streamwise vortices are lifted by the extrusion of the flow along the both sides of the ramp, finally are carried away from the wall, which results in the single streamline on the oil-flow image. From the comparison, it is concluded that the intensity of the streamwise vortices generated from the compression ramp is larger than that from the expansion ramp, and the streamwise vortices are fully curled up not far away downstream of the injector.

Fig. 8 gives the Instantaneous NPLS images expansion ramp injector. From Fig 8.a it is seen that the injected fuel beam expands continuously from the injector orifices, and part of fuel diffuses upstream of the injector. After the injection the fuel mixes with the air flow quickly and it is not definite to distinguish the regular turbulent coherent structures along the interface of the fuel jet with freestream. In this procedure, the broken small structures are the dominated flow structures, which demonstrates that the large structures around the injector orifice have been broken and the small vortices interact with each other and promote the mixing of the fuel with the air flow. Fuel injected jet moves quickly along the air flow direction, and large structures generated in the shear layer between the jet and the airflow quickly are teared up. The fuel quickly diffuses in the main flow and the range of fuel distribution are enlarged continuously. In the rear of the observed window, the fuel has fully mixed with the air flow, and distributes in

most of the internal region. From Fig 8.b it could be seen that fuel mixes with the air flow quickly from the injection location and diffuses along the spanwise direction. From Fig. 8. b, 8. c and 8. d, which give the cross image along different streamwise location, it is seen that the interface of fuel with air flow is very irregular and the streamwise vortex rolling-up could not be clearly identified. The phenomena correspond with the oil-flow image in Fig. 7. a gives the flow structures of the expansion ramp. There exists a shock wave near the ramp corner below the ramp injector, and the shock wave impinges with the streamwise vortices induced by the pressure difference between the bottom surface and the upper surface of the ramp, which promotes the broken-up of the streamwise vortices and blocks the downstream development of the vortices. Fuel diffuses quickly in the fully-developed turbulence. From the figures it is seen that the strongest scattering laser signals, which represents the fuel-concentrated region, increase one by one in the three images along the flow direction. From Fig. 8. d , it is seen that the fuel distributes uniformly in the diffusion region. In summary, the mixing effect of the expansion ramp is dominated by the full-developed turbulence, which demonstrates a finer result.

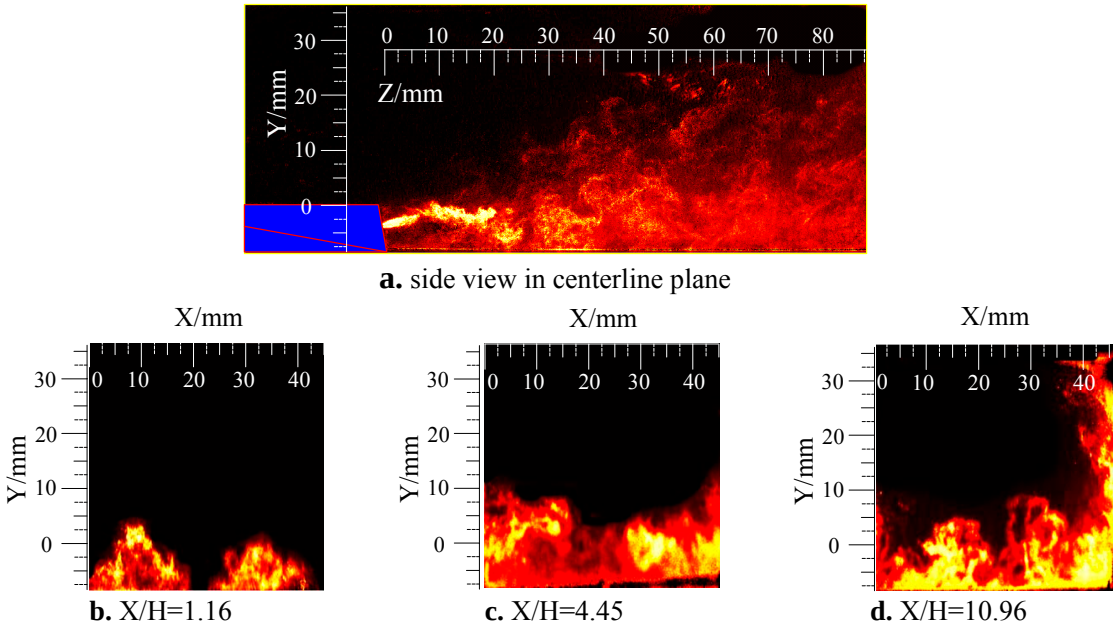

a. side view in centerline plane

b. X/H=1.16 **c.** X/H=4.45 **d.** X/H=10.96

Fig. 8 Instantaneous NPLS images of side view in centerline plane and end view in several streamwise locations of expansion ramp injector

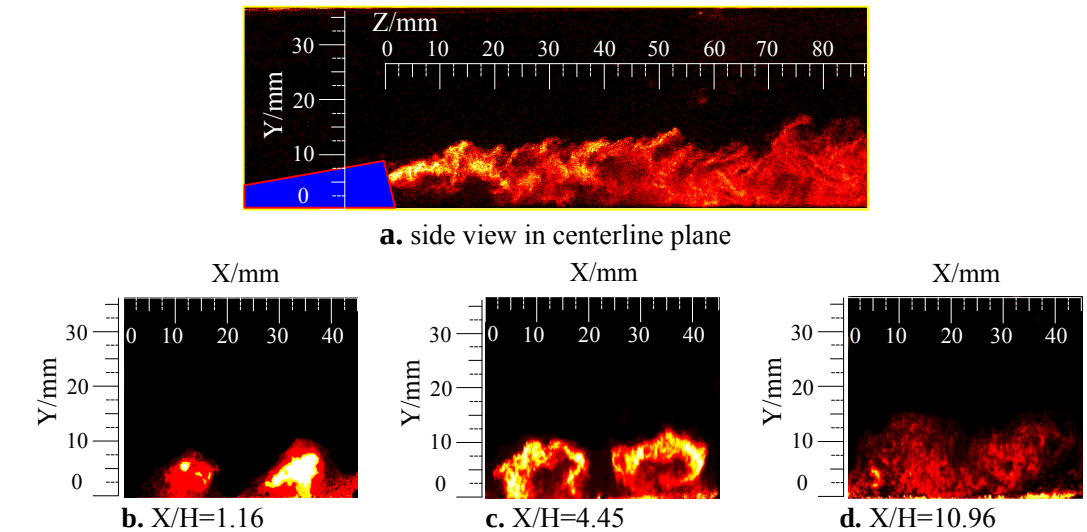

a. side view in centerline plane

b. X/H=1.16 **c.** X/H=4.45 **d.** X/H=10.96

Fig. 9 Instantaneous NPLS images of side view in centerline plane and end view in several streamwise locations of compression ramp injector

Fig. 9 shows the instantaneous NPLS images of side view in centerline plane and end view in several spanwise of expansion ramp injector. From Fig. 9. a , it is seen that the fuel jet expands quickly from the injector orifice, and fuel jet beam seems to become wider. In this procedure, the turbulent diffusion in the shear layer of fuel jet with the main flow dominates the mixing along the streamwise direction. It is seen that this procedure exists in a short distance and the shear layer does not generate large distortion. In the continued procedure, the fuel jet continues to expand and the jet distorts apparently under the effect of the main flow. Contrast to the expansion ramp, obvious large structures are generated in the interface of fuel jet with the airflow. The mixing along the streamwise direction are dominated by the convection of these large structure vortices. And then, the jet shear layer develops gradually and the large structures become to break up. In this procedure the mixing along the streamwise direction is dominated by the diffusion effect of the fully-developed turbulent shear layer. From Fig. 9. b, 9. c and 9. d, the fuel distribution in spanwise and transverse direction could be seen. Compared with the figures in Fig. 6. b which have the same location, it is seen that fuel distribution of the compression ramp in the streamwise plane seems more regular, and the fuel jet is obviously lifted for that the fuel jet has completely gone away from the wall within a not long distance from the injector. However, the fuel jet of the expansion ramp has not been lifted apparently. In Fig. 9. b, the fuel mainly distributes around the axis of the injector and there is almost no fuel in other regions. In Fig. 9. c the pair of counter-rotating streamwise vortices induced by the pressure difference of the ramp surface could be clearly seen. Contrast to Fig. 9. b, the NPLS signals are faint around the injector axis, which is also the kernel of the streamwise vortices, while the signals in surrounding regions are strong. The phenomena reveal that the injected fuel is curled up by the streamwise vortices and carried to the region around the vortices, and the air is engulfed into the kernel of the vortices. Thus the fuel concentration around the jet is relatively high and that of the vortex kernel is relatively low. With the engulfment of the streamwise vortices, fuel mixes with the air sufficiently along the spanwise and transverse direction. Though the distance between location 1 and location 2 is short, from comparisons between the Fig. 9. b and Fig. 9. c, the fuel distribution region from location 1 to location 2 has been obviously enlarged, which demonstrates that the mixing effect in the near field of the compression ramp is mainly dominated by the streamwsie vortices. In this procedure the streamwise vortices have been continuously strengthened and the fuel mixes quickly with the air. From Fig 9. d, it is seen that the intensity of the pair of streamwise vortices has become very faint, which is due to that the fuel jet is lifted and the pair of the streamwise vortices go away from the wall. As the intensity of the streamwise vortices gradually decreases, the mixing effect gradually become weak. The mixing of the fuel with the air is mainly dominated by the turbulent diffusion in the shear layer, which is consistent with the analysis from the centerline symmetric results
.

3.2 Mixing enhancement by the sweepback configuration

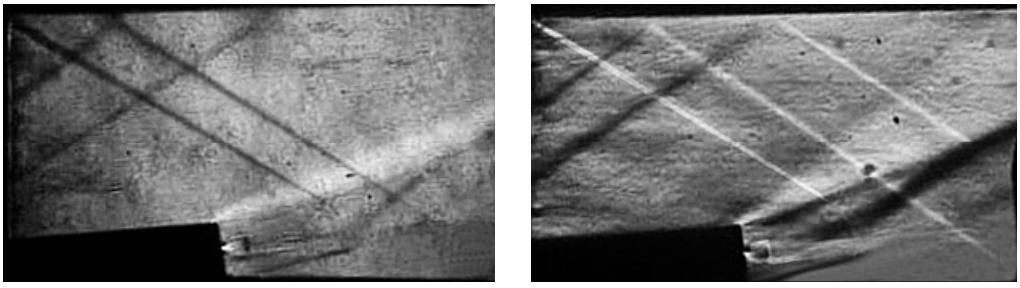

a. Unswept ramp injector **b.** Swept ramp injector

Fig. 10 Schlieren photographs of unswept and swept ramp

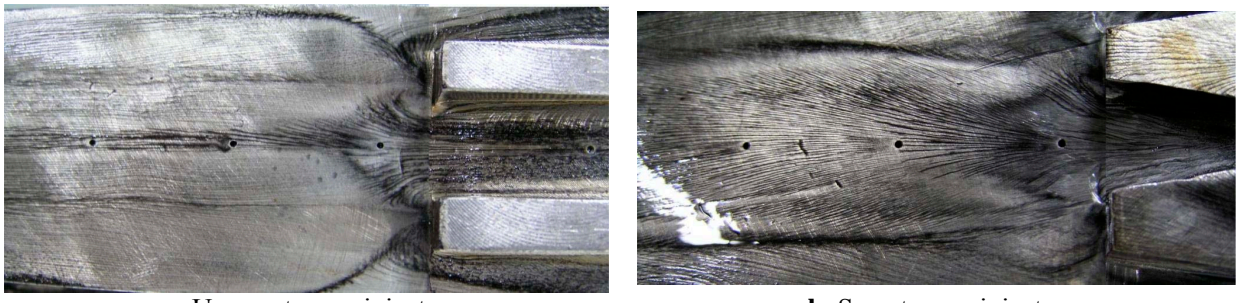

a. Unswept ramp injector **b.** Swept ramp injector

Fig. 11 Oil surface flow pictures of unswept and swept ramp injector

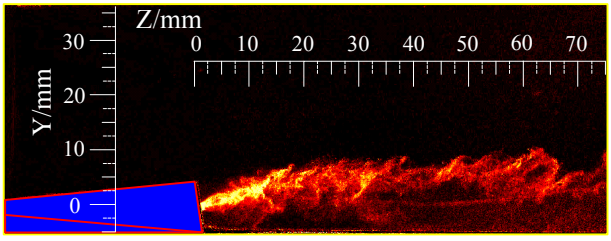

a. side view in centerline plane

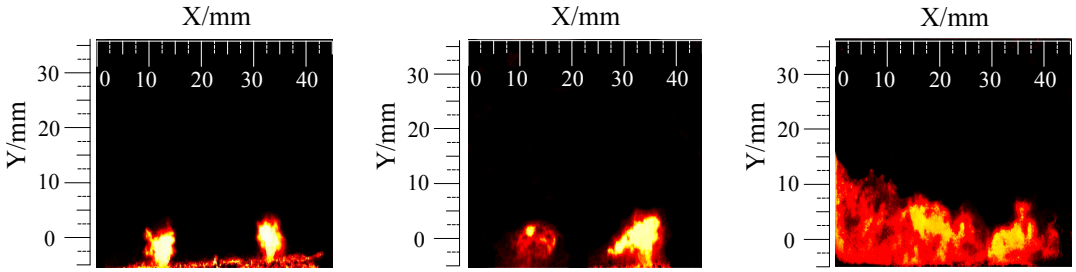

b. X/H=1.16 **c.** X/H=4.45 **d.** X/H=10.96

Fig. 12 Instantaneous NPLS images of side view in centerline plane and end view in several streamwise locations of unswept ramp injector

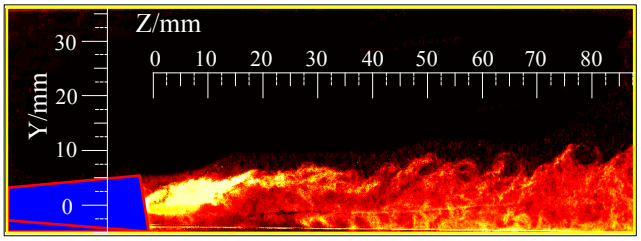

a. side view in centerline plane

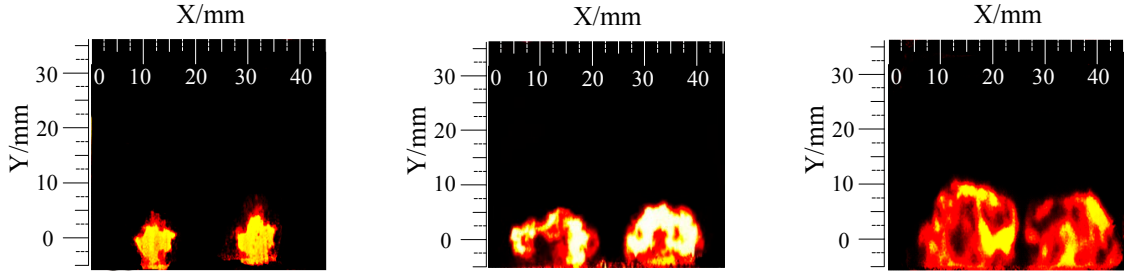

b. X/H=1.16 **c.** X/H=4.45 **d.** X/H=10.96

Fig. 13 Instantaneous NPLS images of side view in centerline plane and end view in several streamwise locations of swept ramp injector

Schlieren photographs of unswept and swept ramp are shown in Fig. 10. In Fig. 10. a and 10. b, the oblique shock wave originating at the leading edge of the ramp and the jet Mach disk are clearly seen. The flowfield structure of the two ramps are very similar except an oblique shock located at the boundary of expansion waves on top of the swept ramp. The oblique shock ,which has an important impact on lifting the injection plume of swept ramp, is emanated from collision between the core supersonic crossflow and the fluid which expand rapidly, accelerate axially and radially toward the centerline when passing through the sweep configuration of the swept ramp.

Fig. 11 displays oil surface flow pictures of unswept and swept ramp injector. Clearly noticeable difference can be revealed when compared with the two pictures. The injection plume downstream of the swept ramp is basically departed from the bottom wall, merely contacting with it at injection centerline plane. Contrary to the swept ramp, the injection plume downstream of the unswept ramp contact with the bottom wall all the while. It can be illuminated that the sweep configuration can lift the injection plume effectively and consequently enhance the fuel–air mixing rate greatly.

Fig. 12 gives instantaneous NPLS images of unswept ramp injector. Overall, the characteristic flow patterns displayed in Fig.12. a show a fair agreement with oil surface flow picture. The injection plume is distorted by streamwise vortices and divorced from the bottem wall of chamber in centerline plane. Mixing along streamwise direction is dominated by turbulent diffusion in less development supersonic mixing shear layer, which grows slowly because of the high velocity of supersonic main flow. From the comparison of Fig. 12. b and Fig. 12. c, it can be seen that the fuel distribution has little change from location 1 to location 2, and the fuel concentrate around the injection port. In this stage, the mixing in spanwise direction is dominated by streamwise vortices originated from ramp, which implies that the streamwise vortices generated by the unswept ramp are weak and grow slowly.

Fig. 13 show instantaneous NPLS images of side view in centerline plane and end view in several spanwise locations of swept ramp injector. From Fig. 13 a, we can see that fuel diffuses quickly in a short distance after injecting from injection port, which has a good agreement with oil surface flow picture. The injection plume is extruded and basically departed from the wall, which can also be seen from Fig. 13. b-d. Mixing along streamwise direction can be divided into two procedures. In the first procedure, the jet beam is injected and under-expanded, and supersonic shear layer is formed because of the discrepancy in velocity between jet and main flow, the mixing in the procedure is poor and dominated by turbulent diffusion in less development shear layer. In the second procedure, the interface of the jet beam is significantly distorted by supersonic inflow and intermittent eddies are originated, and the mixing in this stage is better and dominated by the transport of large eddies.

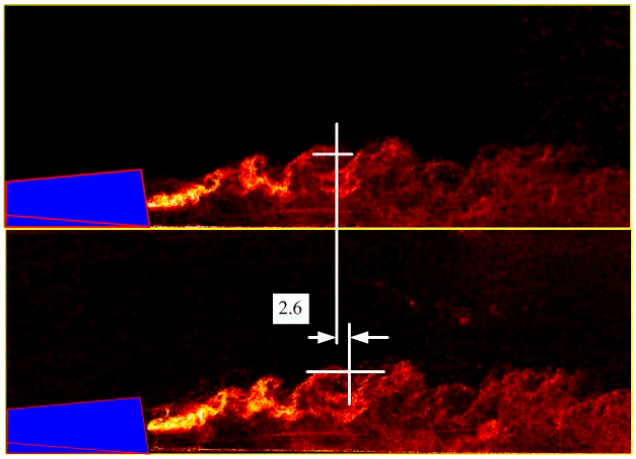

Fig. 14 Two consecutive NPLS images of a side view in the center-line plane of swept ramp, time interval between images $\Delta t = 5\mu s$

Fig. 14 gives two consecutive NPLS images of a side view in the center-line plane of swept ramp, time interval between images is $5\mu s$. It can be seen that the large eddy moves forward 2.6mm during interval of 5 us, and does not change any more in shape, from which we can figure out that the velocity of the large eddy is about 520m/s. It can be illuminated that the jet shear layer of swept ramp has property of fast movement and slow change. The mixing effect along the streamwise direction is dominated by the large eddy in further field of swept ramp.

3.3 Mixing enhancement by the reflected oblique shock

Fig.15. Overprinting of schlieren and NPLI images

Fig.15 show the overprinting of schlieren and NPLS images，it can be seen clearly that the oblique shock wave originating at the leading edge of the ramp is reflected by the top wall of the combustor and then projects onto the fuel injection plume. The mixing enhancement strategy by the reflected oblique shock in the flowfield of ramp injector can be illuminated as two different mechanism.

One is the so-called shock-enhanced mixing mechanism, in which the interaction between the mixing layer and the oblique shock creates strong axial vortices that stretch the fuel/air interface. The interaction of a mixing layer composed of two streams of different densities with an oblique shockwave induces a misalignment between the density gradient in the mixing layer and the pressure gradient of the shockwave. The Helmholtz vorticity transport equation

$$\rho \frac{d}{dt}\left(\frac{\omega}{\rho}\right) = \frac{1}{\rho^2}\nabla\rho \times \nabla P$$

, where the right hand is the variety of vorticity, which is caused by misalignment of density gradient and pressure gradient. The fuel injection plume is distorted by streamwise vortices , which is originated from shock wave, and species concentration gradient along with fuel-air interfacial area increase, i.e. macrocosmic mixing is enhanced. On the basis of this, molecular diffuses quickly and microcosmic mixing enhancement is promoted. On the other hand, the interaction of streamwise vortices generated by the ramp and reflecting oblique shock causes large eddies breaking up, and recirculation is formed which can enhance mixing between fuel and main flow. Large eddies can break up easily when shock wave contacts with streamwise vortex, because pressure gradient is large when crossing shock wave. If the intensity of oblique shock is large enough and streamwise vortices are unstable, large eddies will break up and mixing enhancement can be reached effectively.

4 Summary and Conclusions

Advanced diagnostic tools have been used to study the mixing processes that occur in ramp injectors for supersonic combustion applications. From the experimental work undertaken, the following conclusions can be drawn:

1. NPLS, a novel flow field visualization method, which is more precise and veracious for three-dimensional supersonic flow visualization, is employed in experimental studies on ramp injectors in supersonic flow successfully.
2. Combining NPLS with other visualization methods, the mixing enhancement mechanisms of ramp injectors are discussed. Comparisons of expansion and compression ramp indicate that the completely developed turbulent diffusion dominants the mixing process of expansion ramp, which leads to better mixing effect, especially in the far-

field. As to compression ramp, the near-field mixing is dominated by the entrainment of streamwise vortices .

3. Sweepback configuration strengthens the streamwise vortices greatly. The near-field mixing, which is relatively slow, is dominated by the turbulent diffusion in the shear layer, while the far-field mixing mainly owns to the transport effects of the large-scale spanwise vortices . For unswept ramp injector, mixing along streamwise direction is dominated by the slowly developing supersonic shear layer, which is weaker than that of swept ramp.
4. The reflected oblique shock projecting onto the injection plume can intensify mixing effectively.

5 Acknowledgments

This work is supported by National Science Fund of China, grant number 50906098.

6 References

[1] E. T. Curran, Murthy, S. N. B. Scramjet Propulsion. Volume 189. Progress in astronautics and aeronautics, AIAA 2002.

[2] D. M. Bushnell, Hypervelocity Scramjet Mixing Enhancement, Journal of Propulsion and Power, Vol. 11, No. 5

[3] Mark R. Gruber, Campbell D. Carter, Daniel R. Montes, Lane C. Haubelt, Paul I. King, Kuang-Yu Hsu, Experimental Studies of Pylon-Aided Fuel Injection into a Supersonic Crossflow, Journal of Propulsion and Power, Vol. 24, No. 3, May–June 2008

[4] Donohue, J.M., Victor, K. G., and McDaniel, J. C., Computer-Controlled Multi-Parameter Mapping of 3D Compressible flowfields Using Planar Laser-Induced Iodine Fluorescence, AIAA Paper 93-0048, Jan. 1993

[5] R.J.Hartfield,.Hollo, J.C.McDaniel. Experimental investigation of a supersonic swept ramp injector using laser-induced iodine fluorescence. Journal of Propulsion and Power, 1994, 10 (1) : 129-135

[6] Ian A. Waitz, Frank E. Marblet, Edward E. Zukoski, Investigation of a Contoured Wall Injector for Hypervelocity Mixing Augmentation, AIAA Journal Vol. 31, No. 6, June 1993

[7] James M. Donohue, James C. McDaniel Jr., Hossein Haj-Hariri, Experimental and Numerical Study of Swept Ramp Injection into a Supersonic Flowfield, AIAA Journal Vol. 32, No. 9, September 1994

[8] Diana D. Glawe, Mo Samimy, Abdollah S. Nejad, Tzong H. Chen, Effects of Nozzle Geometry on Parallel Injection into a Supersonic Flow, Journal of Propulsion and Power Vol. 12, No. 6, November-December 1996

[9] T. M.Abdel-Salam, S. N.Tiwari, T. O.Mohieldin. Effects of ramp swept angle in supersonic mixing. AIAA Paper 2000-2377

[10] T. M.Abdel-Salam, S. N.Tiwari, T.O.Mohieldin. Dual-mode flowfield in scramjet combustor. AIAA Paper 2001-2966

[11] A. KONDO, H. HAYASE, S. SAKAUE, T. ARAI, Effect of Expansion Ramp Angle on Supersonic Mixing using Streamwise Vortices, AIAA Paper 2009-127

[12] Vivek Ahuja, Dr. Roy J. Hartfield, Optimization of Fuel-Air mixing for a Swept Ramp Scramjet Combustor Geometry using CFD and a Genetic Algorithm, AIAA Paper 2009-5195

[13] Zhao Y X, Yi S H, Tian L F, Cheng Z Y. Supersonic Flow Imaging Via Nanoparticles. Science in China Series E: Technological Sciences, 2009, 52 (4):922-927

7 Copyright Statement